Int. J. Appl. Math. Comput. Sci., 2018, Vol. 28, No. 4, 745–757
DOI: 10.2478/amcs-2018-0057

PERSONAL IDENTIFICATION BASED ON BRAIN NETWORKS OF EEG SIGNALS

WANZENG KONG [a,*], BEI JIANG [a], QIAONAN FAN [a], LI ZHU [b,c], XUEHUI WEI [a]

[a]College of Computer Science
Hangzhou Dianzi University, Hangzhou, 310018 China
e-mail: kongwanzeng@hdu.edu.cn

[b]School of Information Science and Engineering
Xiamen University, Xiamen, 361005 China
e-mail: zhulibrain@gmail.com

[c]Laboratory for Advanced Brain Signal Processing
BSI, RIKEN, Wako, Saitama, 351-0198 Japan

Personal identification is particularly important in information security. There are numerous advantages of using electroencephalogram (EEG) signals for personal identification, such as uniqueness and anti-deceptiveness. Currently, many researchers focus on single-dataset personal identification, instead of the cross-dataset. In this paper, we propose a method for cross-dataset personal identification based on a brain network of EEG signals. First, brain functional networks are constructed from the phase synchronization values between EEG channels. Then, some attributes of the brain networks including the degree of a node, the clustering coefficient and global efficiency are computed to form a new feature vector. Lastly, we utilize linear discriminant analysis (LDA) to classify the extracted features for personal identification. The performance of the method is quantitatively evaluated on four datasets involving different cognitive tasks: (i) a four-class motor imagery task dataset in BCI Competition IV (2008), (ii) a two-class motor imagery dataset in the BNCI Horizon 2020 project, (iii) a neuromarketing dataset recorded by our laboratory, (iv) a fatigue driving dataset recorded by our laboratory. Empirical results of this paper show that the average identification accuracy of each data set was higher than 0.95 and the best one achieved was 0.99, indicating a promising application in personal identification.

Keywords: EEG, personal identification, brain network, phase synchronization.

1. Introduction

Personal identification is becoming a key point of personal information security (Huang *et al.*, 2012). Traditional personal identification methods are faced with the risk of being copied or forged easily (e.g., keys, ID cards and passwords). Hence, biometric methods appear to be more reliable for identification. Biometrics including DNA, fingerprint, face, voice-print and iris had been widely used in identifying people in the last decades (Jain *et al.*, 2005; Pujol *et al.*, 2016). However, there are still risks of those being forged. Researches showed that fake fingerprints made of gelatin could easily cheat the fingerprint identification system. Iris recognition systems also find it difficult to distinguish false iris features etched on contact lenses from genuine ones. EEG has advantages of stability, uniqueness and being hard to imitate. In these virtues, EEG as a new biometric tool for personal identification has gradually increased people's attention in recent years.

Previous studies showed that EEG could be used for personal identification. Armstrong *et al.* (2015) first proposed the concept of "brainprint." They put forward that brainprint referred to a unique and durable biometric, which was generated by the brain and could be used for personal identification. Paranjape *et al.* (2001) recorded EEG signals in resting state and used an autoregressive (AR) model for identification using 40 subjects. The classification accuracy was higher

*Corresponding author

than 80%. Poulos *et al.* (1999) performed personal identification experiments based on parametric spectral analysis of the alpha rhythm. The results showed that the EEG carried genetic information. The classification accuracies of the experiments were in the range of 72% to 84%. Das *et al.* (2009) used rapid visual evoked EEG activities to analyze the data involved in a visual perceptual task. They adopted discriminative spatio-temporal filters to extract features and classified 20 subjects with LDA and support vector machines (SVMs), which achieved recognition rates ranging from 75% to 94%. Yeom *et al.* (2013) proposed a novel method in which people who were confronted with self-face and a non-self-face would provide different performance, which can be measured by EEG. They used the EEG recordings for personal authentication and the mean accuracy rate was 86.1%. Maiorana *et al.* (2015) defined the meaning of eigenbrains and eigentensorbrains by principal component analysis (PCA) and multilinear PCA (MPCA). During the experiment, the EEG of 30 subjects was recorded from the resting state. They used LDA for classification and got the accuracy of 87.9%.

Although these studies provided evidence to consider EEG as a powerful tool to assess personal identification, the amplitude information of signals was only used. It is easily influenced by random factors. To some extent, deviation is inevitable if amplitude information is used in experiments. There is a close relationship between cognitive brain activity and synchronization of neurons (Hebb, 2013). Nevertheless, if synchronization does not show the amplitude relationship, the method based on the amplitude will not comprehensively analyze the information of EEG signals. Phase synchronization analysis can avoid these defects, as it analyzes the interrelation between EEG pairs based on phase and synchronization angles. It ignores the effect of amplitude, but calculates using the instantaneous phase between the signals, which is more stable.

In the last few years, it was proved that phase synchronization in chaotic systems could be applied to biological sciences. Moreover, it could be also used to confer the functional connectives of EEG signals. Phase synchronization was widely used in physiological research. It is assumed that a functional network could be made up by a coherent electrophysiological activity which could span multiple brain regions (Fries, 2005). Brain networks based on EEG phase synchronization were often used for observation and prediction of diseases. Ling *et al.* (2015) employed the phase synchrony index matrix to construct brain networks. They found that patients had a further loss of small-world attribute than healthy people. Jamal *et al.* (2015) extracted synchrostate properties from EEG signals and then utilized them to measure phase synchronization to generate the brain connectivity graph. However, processing on a specific task-based dataset was a common way to validate their hypothesis. The main reason was that the method they used could only effectively process a single type of EEG data. In the experiments, subjects always performed one specific type of task or had to stay in a regular environment (Su *et al.*, 2010).

In this paper, we introduce a methodology that could be used for EEG-based personal identification with phase synchronization analysis. Brain functional networks constructed with phase synchronization values are used for personal identification. The connectivity matrix, generated by the phase locking value (PLV) matrix, would create a weighted undirected network. Then, we utilize combined attributes of the network including the degree of a node, the clustering coefficient and the global efficiency to represent each person. The calculation method of these attributes is related to the work of Rubinov and Sporns (2009) as well as Vukašinović *et al.* (2014). These attributes represent the activity of the brain. The features composed of these attributes would be a good representation for personal identification. In contrast to related works, our method applied phase synchronization of EEG signals, rather than amplitude information. Phase synchronization of EEG signals could describe a relation which may exist between two channels. The proposed method is evaluated on four different data sets from different tasks, in contrast to just one type of EEG signals from one task. Two of the data sets were public data sets, the other two were collected by our lab.

This paper is structured as follows. In Section 2, we introduce the method of constructing the brain network and classification. In Section 3, we analyze the attributes of the brain network as features for personal identification. In Section 4, experimental results and analysis of classification in different wave bands are presented. The last section present conclusions.

2. Method

2.1. Preprocessing. EEG is a non-stationary signal. A copious amount of external noise will affect EEG recording. Preprocessing raw EEG can minimize disturbances of other noise signals. In our experiments, EEG data were filtered between 2 Hz and 47 Hz. The value of each channel was dealt with using the common average reference (CAR) method (McFarland *et al.*, 1997). Then, Butterworth band-pass filters were used to select the corresponding band.

2.2. Phase synchronization. Phase synchronization is a new way to analyze EEG signals. It can inhibit the impact of amplitude and retain phase components of EEG signals. Phase synchronization is quantified by the phase locking value (PLV).

The PLV of two continuous time series $x(t)$ and $y(t)$ is calculated as follows:

$$\text{PLV} = |\langle \exp(j\{\Phi_x(t) - \Phi_y(t)\})\rangle|, \tag{1}$$

where $\langle \cdot \rangle$ means the averaging operator in continuous time t, while $\Phi_x(t)$ and $\Phi_y(t)$ are the respective instantaneous phases of $x(t)$ and $y(t)$ at an instant of time t.

There are two general ways to calculate the instantaneous phase. One is a Hilbert transform and the other is a Gabor wavelet transform (Le *et al.*, 2001). McFarland *et al.* (1997) claimed that there was no much difference between these when processing EEG signals. In this paper, we use a Hilbert transform to calculate the instantaneous phase of EEG signals. The Hilbert transform for a given continuous time series $x(t)$ is

$$\tilde{x}(t) = \frac{1}{\pi} P \int_{-\infty}^{+\infty} \frac{x(t)}{t-\tau}\,\mathrm{d}\tau, \tag{2}$$

where P denotes the Cauchy principal value. It can avoid the appearance of a singular value when $t = \tau$. Here $x(t)$ is described in this way, because the narrow band signal is characterized by a spectrum limited to a narrow frequency range. The envelope and phase changes are slow. Thus $\tilde{x}(t)$ is used to represent $x(t)$.

Then $x(t)$ is defined as

$$Z_x(t) = x(t) + j\tilde{x}(t) = A_x(t)e^{j\Phi_x(t)}, \tag{3}$$

where $A_x(t)$ and $\Phi_x(t)$ are the instantaneous amplitude and the instantaneous phase of $x(t)$, respectively. $\Phi_x(t)$ can be defined as

$$\Phi_x(t) = \operatorname{atan}\frac{\tilde{x}(t)}{x(t)}, \tag{4}$$

and $\Phi_y(t)$ stands for the instantaneous series $y(t)$.

If the phase difference $\Phi_{xy}(t)$ between $x(t)$ and $y(t)$ satisfies

$$\Phi_{xy}(t) = |n\Phi_x(t) - m\Phi_y(t)| \leq \text{const}, \tag{5}$$

where n and m are integers and const represents a constant boundary of instantaneous phase difference, then $x(t)$ and $y(t)$ are called $n : m$ phase synchronization. In the experiments, the value of const was 0.035, the reason why we used this value can be found in the work of Rosenblum *et al.* (1996). $1:1$ phase synchronization is commonly used as a neurobiological signal, for instance, in Kong's research on EEG (Kong *et al.*, 2017). Therefore, $1:1$ phase synchronization is also used in this paper.

According to the value of the instantaneous phase at time t, the PLV of two time series $x(t)$ and $y(t)$ could be calculated (Rosenblum *et al.*, 2012). We selected a one-second time window to compute the PLV of different band signals. There are H non-overlapping time segments of each sample, and the average PLV is the mean of the H seconds phase locking value. Therefore, the average PLV can be written as

$$PLV_{\text{avg}} = \frac{1}{H}\Big|\sum_{h=1}^{H}\langle \exp(j\Delta\Phi)\rangle\Big|, \tag{6}$$

where $\Delta\Phi$ denotes the phase difference between $\Phi_x(t)$ and $\Phi_y(t)$, i.e., $\Delta\Phi = \Phi_x(t) - \Phi_y(t)$, and $h = 1, 2, \ldots, H$ is the number of segments.

We treated every channel as a separate time series and computed phase synchronization for every pair of N EEG signals, obtaining an $N \times N$ symmetric matrix

$$\mathbf{V} = \begin{bmatrix} 1 & v_{12} & \ldots & v_{1n} \\ v_{21} & 1 & \ldots & v_{2n} \\ \vdots & \vdots & \vdots & \vdots \\ v_{(n-1)1} & v_{(n-1)2} & \ldots & v_{(n-1)n} \\ v_{n1} & v_{n2} & \ldots & 1 \end{bmatrix}. \tag{7}$$

The elements v_{ij} represented the average PLV between the i-th and j-th channels. The symmetric matrix $\mathbf{V}$ was used as the connectivity matrix of the brain network, cf. Fig. 1.

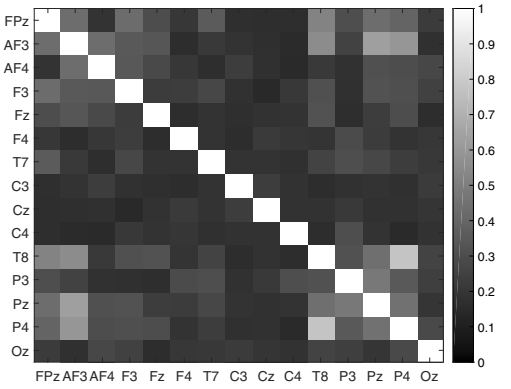

Fig. 1. Symmetric PLV matrix $\mathbf{V}$ with 15 channels. The color scale varies from 0 to 1, and the closer the chroma to 1, the more synchronized the EEG signals between two channels.

2.3. Brain network. The brain network describes the activities among neurons, neuronal clusters and brain areas. There are three types of brain networks related to connectivity: anatomical connectivity, functional connectivity and effective connectivity (Bullmore and Sporns, 2009; Park and Friston, 2013). Methods for measuring functional connectivity may be divided into nonlinear and linear (Stam, 2009). The brain network may be theoretically represented by a graph, and graph theory

could be adopted to analyze it (Sakkalis *et al.*, 2015). The graph is obtained through calculating the connectivity matrix of the brain network.

Furthermore, we used the PLV to calculate functional connectivity. The method of constructing the connectivity matrix was similar to that in the study of Chavez *et al.* (2010). In order to ensure that there was no self-connection, the diagonal of the connectivity matrix was set to zero. According to graph theory, a weighted undirected graph G is generated by the connectivity matrix, where $G = \{N, E, W\}$; N represents a set of nodes of the graph, E is a set of undirected edges between nodes, W is a set of weights that describe the strength of the connections. In order to keep up with the information from phase synchronization, the connectivity matrix does not need to have threshold processing. Then, a fully connected weighted undirected graph G could be obtained.

2.3.1. Network analysis. After computing the PLV, an $N \times N$ weighted undirected graph could be constructed from the connectivity matrix. N equaled the number of EEG channels and every node represented an EEG channel. Each edge meant that there was phase synchronization between two channels. The weights of edge described the strength of phase synchronization. According to graph theory, the attributes of the brain network are important characteristics:

- *Degree of a node.*

  The degree is the most important feature to describe statistical characteristics of nodes in a graph. For a weighted undirected graph G, the degree of a node represents the sum of the weight value ($w_{ij} \in W$) of connecting with others, where w_{ij} is the connection strength between nodes i and j. The degree of node i is defined as below:

$$k_i^w = \sum_{i,j \in N, i \neq j} w_{ij}. \tag{8}$$

- *Global efficiency.*

  The global efficiency of a network describes information transmission efficiency (Lei *et al.*, 2014). A higher value indicates that exchanging information in the network has a lower cost. It is an indicator of the traffic capacity of a network (Boccaletti *et al.*, 2006). The global efficiency is defined as the reciprocal of the harmonic mean of all nodes in the network (Latora and Marchiori, 2001):

$$E = \frac{1}{n-1} \sum_{i \in N} \frac{\sum_{j \in N, j \neq i} \left(d_{ij}^w\right)^{-1}}{n-1}. \tag{9}$$

  In the weighted undirected network, $d_{ij}^w = \sum_{a \in g_{i \leftrightarrow j}^w} f(a)$, where f is a map (e.g., an inverse) from weight to length and $g_{i \leftrightarrow j}^w$ is the shortest weighted path between i and j.

- *Clustering coefficient.*

  The clustering coefficient characterizes the local connectivity of the network (Saramäki *et al.*, 2007). The clustering coefficient of a network is another important parameter of measuring the network. It indicates that a node has many connected nodes. It is defined as

$$C = \frac{1}{n} \sum_{i \in N} \frac{2t_i}{k_i(k_i - 1)}, \tag{10}$$

  where t_i is the geometric mean of triangles around vertex i, $t_i = \frac{1}{2} \sum_{j,h \in v_i} (w_{ij} w_{jh} w_{ih})^{\frac{1}{3}}$; v_i denotes the neighborhood of vertex i, $j, h \in v_i$ (Onnela *et al.*, 2005); k_i denotes the number of edges connected to vertex i.

The feature vector of each sample contained the degree of nodes, the global efficiency and the clustering coefficient. The software to calculate graph theoretical measures can be the Brain Connectivity Toolbox (Rubinov and Sporns, 2009) (`http://www.brain-connectivity-toolbox.net/`).

2.4. Linear discriminant analysis. LDA is a classic pattern recognition algorithm, also called the Fisher discriminant analysis. It is a well-known supervised classifier based on a linear discriminant function (Ye *et al.*, 2004). The basic concept of LDA is to project the sample of high dimension onto the optimal discriminant sub-space (Peng and Lu, 2017). The aim of LDA is to make the distance between classes as great as possible and the distance within class as close as possible (Kim *et al.*, 2003).

For a given sample set, there are M samples in N classes, and each sample is a d-dimensional feature vector. Each feature vector is defined as $x_i = \{x_1^i, x_2^i, x_3^i, \ldots, x_d^i\}$, $i = \{1, 2, \ldots, N\}$. M samples are divided into N classes. The projection function $y = w^T x$ is used to project samples onto a sub-space. According to these results, the samples from different classes can be separated as far as possible. Therefore, the goal is changed to find the best w. For a multi-classification problem, a k-dimensional W is required for projection. The results of samples after projection are expressed as Y. Thus we have $Y = W^T x$.

The mean of each class is defined as

$$m_i = \frac{1}{M_i} \sum_{x \in N_i} x \tag{11}$$

where N_i stands for class i, and M_i signifies the sample numbers of class N_i.

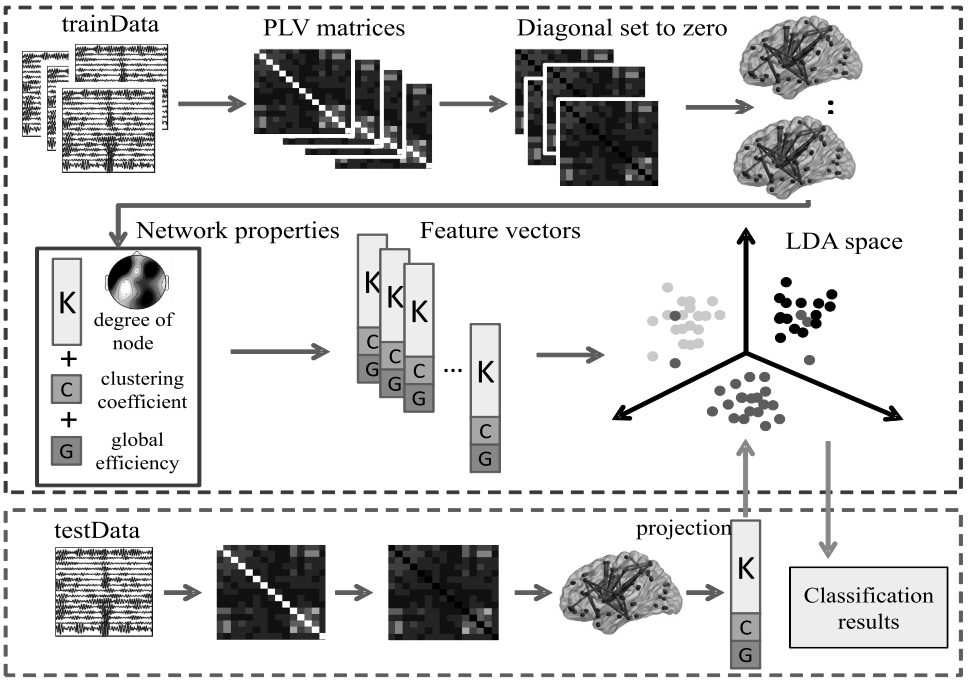

Fig. 2. Specific process of the proposed method.

A matrix that describes the degree of dispersion of all kinds of classes is defined as

$$S_i = \sum_{x \in N_i} (x - m_i)(x - m_i)^T \tag{12}$$

The matrix S_i is called a scatter matrix.

Within-class (S_w) and between-class (S_B) scatter matrices are respectively defined as

$$S_w = \sum_{i=1}^{N} S_i = \sum_{i=1}^{N} \sum_{x \in N_i} (x - m_i)(x - m_i)^T, \tag{13}$$

$$S_B = \sum_{i=1}^{N} M_i (m_i - m)(m_i - m)^T, \tag{14}$$

where N is the number of classes and x are samples, m_i is the i-th class mean, m is the global mean. We define

$$J(W) = \frac{W^T S_B W}{W^T S_w W}. \tag{15}$$

The discriminant criterion is $\arg\max_w J(W)$. The solution process for W proceeds as follows:

$$\begin{cases} W = \arg\max_w J(W) = \arg\max_w \frac{W^T S_B W}{W^T S_w W}. \\ \text{such that} \qquad W^T S_w W = c \neq 0 \end{cases} \tag{16}$$

A Lagrange multiplier is introduced to calculate the maximum of $W^T S_B W$; then the problem is changed to resolve the following issue:

$$L(w_i, \lambda) = {w_i}^T S_B w_i - \lambda({w_i}^T S_w w_i - c). \tag{17}$$

The condition of getting an extremum of the formula (16) is that the derivative of w_i is zero. Thus,

$$S_B w_i = \lambda S_w w_i, \tag{18}$$

and then

$$S_w^{-1} S_B w_i = \lambda w_i. \tag{19}$$

W is a matrix that consists of feature vectors corresponding to k generalized feature values of $S_w^{-1} S_B$, where $k \leq N - 1$. Thus W was obtained, where $W = \{w_1, w_2, \ldots, w_k\}$.

After projecting the EEG data onto a sub-space, the nearest neighbor rule was used for classification.

2.5. Summary of the proposed method. In this paper, the average PLV was used as the weight of brain functional network connectivity. The brain network attributes were combined as feature vectors for personal identification. The detailed steps were as follows (see Fig. 2):

Step 1. Raw EEG data were obtained from experimental data sets. All data were preprocessed and filtered to four bands.

Step 2. The PLV of the preprocessed EEG data was calculated for each one-second segment. H non-overlapping time segments (one second as a time

segment) were taken as a sample. The average PLV was computed to get an $N \times N$ symmetric matrix V.

Step 3. The symmetric matrix V was used as the connectivity matrix of brain network to weigh brain network functional connectivity. The diagonal elements of the matrix V were set to zero to avoid self-connection, which was labeled as $V^{'}$. Then the brain functional network was represented as a weighted undirected graph G by the matrix $V^{'}$.

Step 4. The attributes including the degree of nodes, the clustering coefficient and the global efficiency of brain network for each sample were computed. A feature vector combined these attributes was used for classification.

Step 5. The LDA projection space was trained by training data. Test data were projected to the LDA projection space, and the category of the test sample was determined by the nearest neighbor rule.

3. Experiments

In this paper, four data sets were used for personal identification. Differences in the accuracies in beta, gamma, alpha and theta bands were discussed. For each dataset, 480-second raw data of each subject were recorded. The data were partitioned using a 30-second window segment without overlapping to calculate the mean PLV matrix. The attributes of the brain network were combined as a feature vector of each sample. Therefore, there were 16 samples collected from each subject. The attributes contained the degree of the node, the global efficiency and clustering coefficient. The samples of each subject were averagely assigned to training dataset and the test dataset. Then the LDA classifier was used for classification.

3.1. Data acquisition. Four datasets were used in this paper. Two of them were international public data sets. In the following context, we referred to them as BCI data and Motor data. The other two were recorded by our laboratory. The one collected through a neuromarketing experiment would be referred to as NMK data. The other one, collected from a complex task during a fatigue driving experiment, would be referred to as DRI data.

3.1.1. BCI data. The dataset was obtained from BCI Competition 2008—Graz data set A (Brunner *et al.*, 2008). The dataset contained EEG data recorded from 9 subjects. Each subject undertook four different motor imagery tasks: left hand (class 1), right hand (class 2), both feet (class 3), and tongue movements (class 4). For each subject, 2 sessions of data were recorded. Each session was composed of 6 runs. Participants took a short break between each run. One run consisted of 48 trials (12 for each of the four possible classes), yielding a total of 288 trials per session. The sampling frequency of EEG data was 250 Hz. There were 22 EEG channels and 3 EOG channels. In our experiment, we used only 22-channel EEG data. The montage of BCI data is indicated in Fig. 3.

3.1.2. Motor data. The Motor data is a public dataset obtained from the BNCI Horizon 2020 project. It is a two-class motor imagery task data set recorded by Steyrl *et al.* (2016). There were 14 participants in the experiment. The paradigm was based on the training paradigm of the cue-guided Graz BCI (Pfurtscheller and Neuper, 2001). The session consisted of 8 runs, 5 of them for training and 3 feedback for validation. Here, we just used the 5 runs for training as our experiment data set. One run was composed of 20 trials. Participants performed 5-second imaginative movements of the right hand and feet. EEG signals were recorded with a biosignal amplifier. The data were sampled at 512 Hz. The montage of Motor data is indicated in Fig. 4.

3.1.3. Neuromarketing data. The NMK data were recorded from an experiment with 20 subjects (Kong *et al.*, 2013). Subjects were equally divided into men and women. They were all healthy and had no personal history of neurological disorders. The stimulus was a ten-minute video, which was composed of a neutral video (8 minutes) and 6 advertising video clips (around 30 seconds) interspersed into the neutral video. During the experiment, the subjects sat in a quiet room, passively experimenting stimuli, and were instructed to look at the screen in front of them. They knew little about the purpose of the experiment. The EEG data were recorded by 16-channel G-Tec equipment and the sampling frequency was 256 Hz. The montage of the experiment was shown in Fig. 5. The red electrodes were selected for utilization in our experiment.

3.1.4. Fatigue driving data. The DRI data were recorded through a fatigue driving experiment (Kong *et al.*, 2015). This experiment included 12 subjects aged between 23 and 25. All the subjects held a driver's licence. Each subject was right side dominant and had no history of neurological or psychiatric disorders. A simulation driving system with an imitation cab was used. During the experiment, there were 8 different conditions. The subjects had to drive under these conditions with the priority of the driving control. The EEG data were recorded by a 16-channel G-Tec equipment at the sampling rate of 256 Hz, and the impedances were kept below 5 kΩ.

3.2. Attribute analysis. In order to verify that the attributes of the brain network can be used as indices for

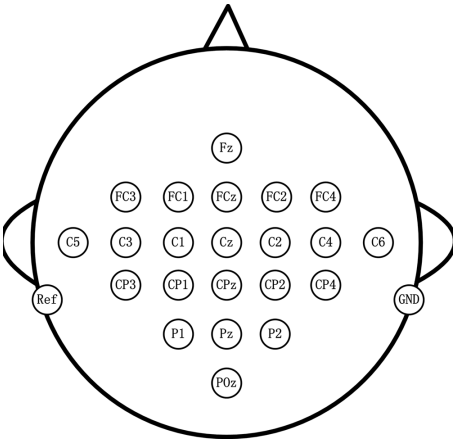

Fig. 3. EEG montage of the BCI data.

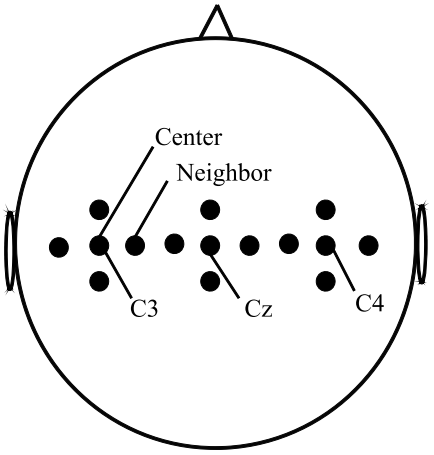

Fig. 4. Small Laplacian electrode placing scheme centered at C3, Cz, and C4. Distances between neighboring electrodes are 2.5 cm.

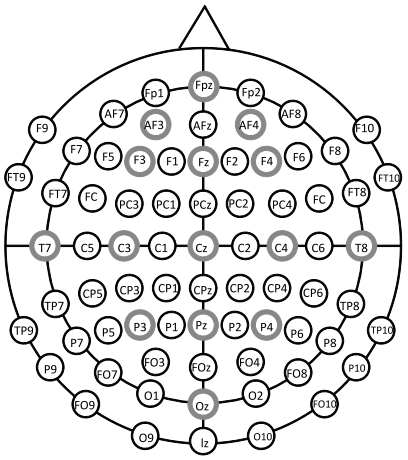

Fig. 5. EEG montage of the NMK data.

personal identification, the degree of the node, the global efficiency and the clustering coefficient were presented. Topographic maps of brain and other mathematical statistics forms were used to show the attributes of the brain network.

3.2.1. Degree of a node. For the brain network, each node had a degree, which was discussed in Section 2. For the sake of generating a brain network, an EEG channel was used as a network node. The brain topographic map for each subject was presented through the mean values of nodes in the EEG signal. In this section, the BCI, NMK and DRI data were taken as examples (see Figs. 6–8). For the Motor dataset, as shown in Fig. 4, there was no direct mapping of the electrodes in that data set on the 10–20 system except for the positions C3, Cz, C4. The others were in between 10–20 system electrodes. Their system was equidistant. All electrodes had a distance of 2.5 cm from the surrounding. Hence we could not show brain topographic maps of the Motor dataset.

Figures 6, 7 and 8 represented brain topographic maps for BCI, DRI and NMK dataset respectively. As shown in the figures, the connection strength exhibited a certain symmetry between the left and right hemisphere for each subject. However, the distribution of the connection strength for each subject showed significant differences. The brain topographic maps for the DRI data are shown in Fig. 7. In the fatigue driving experiment, subjects were required to execute relatively complex tasks. When facing the same problem, people with different levels of knowledge or habits would have different responses. Therefore, there were differencies in their thinking process (e.g., the cognitive process of the brain). As shown in Fig. 7, the maps of some subjects varied between each subjects while some subjects' maps (subjects 5 and 9) were similar.

In order to verify the robustness of the degree of a node as the index for personal identification, we selected 4 epochs of 12 subjects in the DRI to draw the brain topographic maps which are shown in Fig. 9.

As presented in Fig. 9, there was an evident similarity between the brain's connection strength in different epochs of the same subject. However, there was a discrepancy for different subjects.

In order to make the experiment more persuasive, we performed a statistical analysis on the degree of nodes. The BCI dataset was taken as an example. We calculated the mean vector of the degree of nodes from 9 subjects and 1 mean vector represented a subject. After that the covariance matrix of the 9 subjects was calculated. The results are shown in Fig. 10.

As presented in Fig. 10, we could see that there were differences in the degree of nodes among individuals.

3.2.2. Global efficiency and the clustering coefficient. The global efficiency and the clustering coefficients are two necessary elements of the feature vector. To further explore their influence and performance, we showed

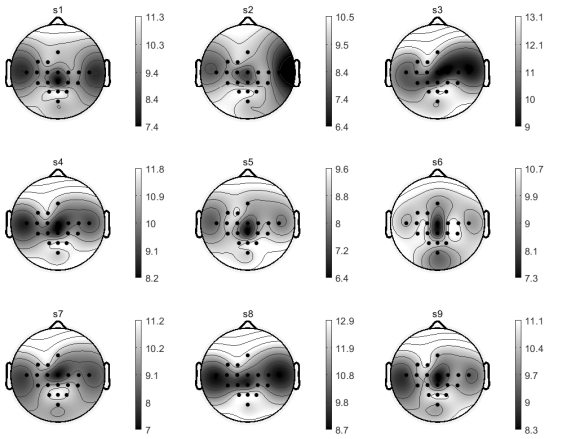

Fig. 6. Brain topographic map of four-class motor imagery tasks in the BCI Competition 2008 (BCI dataset). The black dots denote the EEG channel location while the light color and the deep color stand for the mean value of the degree of a node for each EEG channel.

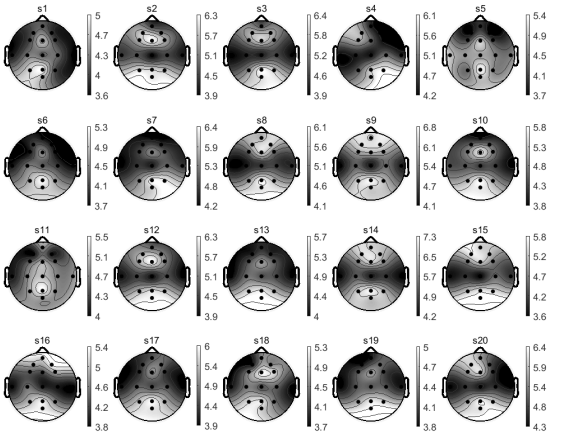

Fig. 8. Brain topographic map for a neuromarketing cognitive task recorded by our laboratory (NMK dataset). The black dots denote the EEG channel location while the light color and the deep color stand for the mean value of the degree of a node for each EEG channel.

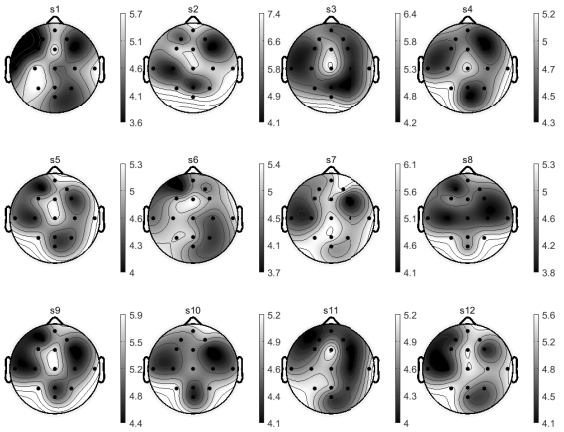

Fig. 7. Brain topographic map for a fatigue driving dataset recorded by our laboratory (DRI dataset). The black dots denote the EEG channel location while the light color and the deep color stand for the mean value of the degree of a node for each EEG channel.

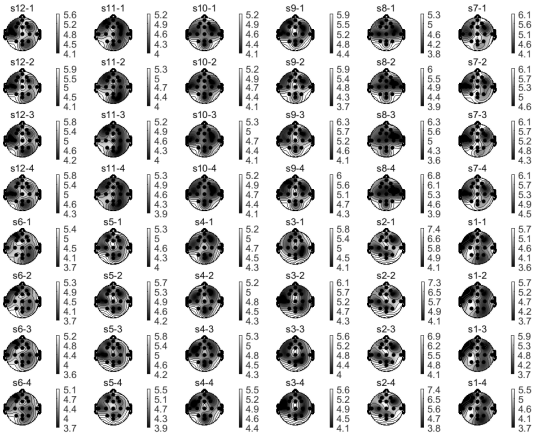

Fig. 9. Brain topographic map of mean value of nodes for four epochs for a fatigue driving dataset recorded by our laboratory (DRI dataset). The black dots denote the EEG channel location while the light color and the deep color stand for the mean value of the degree of a node for each EEG channel.

the relationship between the global efficiency and the clustering coefficient of each subject in the form of a scatter diagram (see Fig. 11). The global efficiency was the x-axis and the clustering coefficient was the y-axis.

Figure 11 described the relationship between the global efficiency and the clustering coefficient of each dataset. In the subfigures, each subject had a relatively unique distribution. The linear fitting of the global efficiency and the clustering coefficient was made. We found that the relationship value between two subjects was different. This phenomenon also proved that the global efficiency and the clustering coefficient had a specific representation of individuals. Moreover, from the result of linear fitting, we found that the global efficiency and the clustering coefficient of each sample were close to a proportional relation. According to Latora and Marchiori (2001), the clustering coefficient could be seen as first approximations of efficiency evaluated on a local scale. The local efficiency was the global efficiency computed in the neighborhood of the node (Rubinov and Sporns, 2009). The weighted local efficiency broadly parallelled the weighted clustering coefficient (Onnela *et al.*, 2005). Therefore, we think that the clustering coefficient and the global efficiency had a similar variation tendency to some extent, which was consistent with our experiment's results.

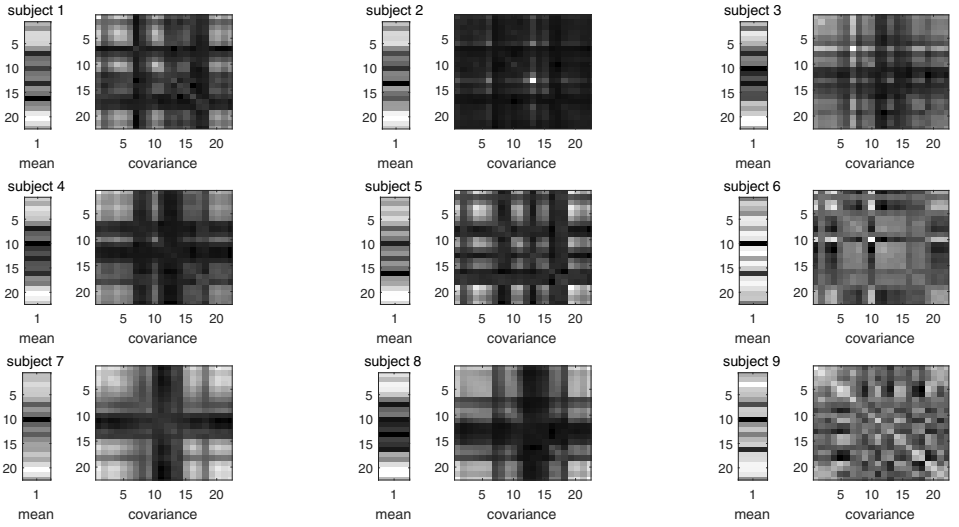

Fig. 10. Mean vector and the covariance matrix of four-class motor imagery tasks in the BCI Competition 2008 (BCI dataset).

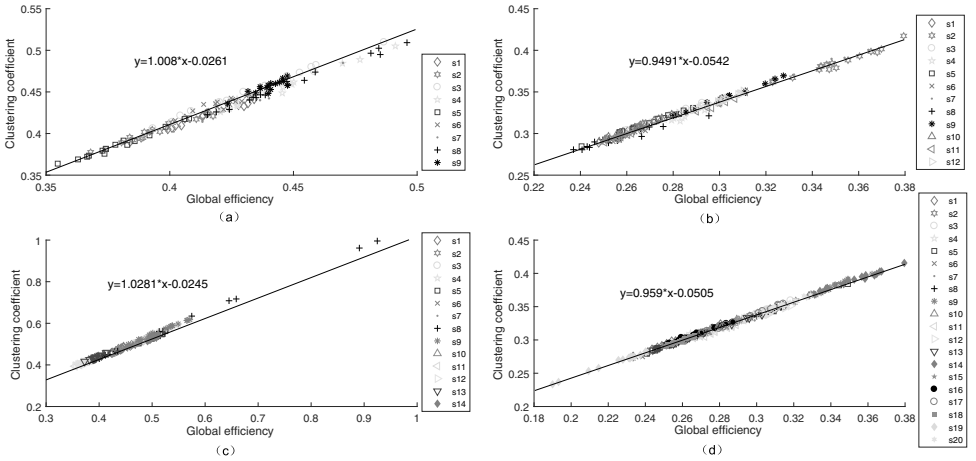

Fig. 11. Relationship between the global efficiency and the clustering coefficient: BCI data (a), DRI data (b), Motor data (c), NMK data (d).

4. Results of experiments

4.1. Results analysis based on four bands. Brain waves were spontaneous rhythmic electrical activities. Generally, they could be divided into four bands as theta (4–8 Hz), alpha (8–13 Hz), beta (13–30 Hz) and gamma (30–40 Hz) bands. The EEG signal intensities were different in the four bands when people were in different states. Therefore, we made a comparison among subband data to explore in which band the attributes from brain network would exhibit better performance in personal identification. For each data set, we adopted 10 times 2-fold cross validation and drew a line chart of classification accuracies in four bands. Figure 12 shows mean classification accuracy results per dataset per band.

As shown in Fig. 12, the accuracies of the beta band, alpha band and gamma band data were higher than those of the theta band across the four data sets. Except for one time in Motor data, the classification accuracy in the theta band was always lower than the other three bands. According to the results of this experiment, we thought that in beta and gamma bands the attributes of the brain network had better performance in personal identification.

4.2. Efficiency of combined attributes. We compared the efficiency of single attribute with that of combined attributes. The latter gave a better estimate for classification in personal identification. Experiments were carried out on the four data sets.

Table 1 demonstrates that the combined attributes as a feature of personal identification could yield better performance. For four data sets, when a single attribute was used as a feature, the classification accuracy rate was

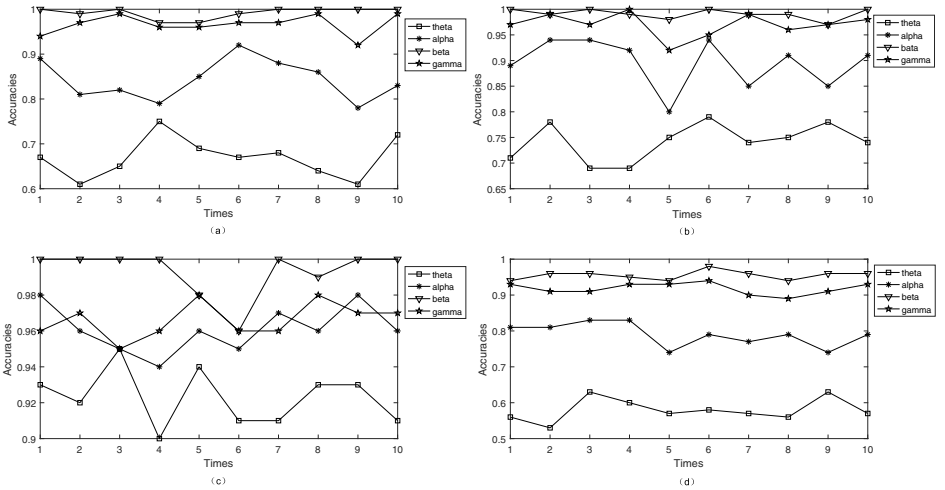

Fig. 12. Four bands classification accuracies for four datasets: BCI data (a), DRI data (b), Motor data (c), NMK data (d).

Table 1. Classification results of different features.

datasets / attributes	BCI data	DRI data	NMK data	Motor data
D	0.980	0.986	0.945	0.991
D+Eg+C	**0.992**	**0.991**	**0.956**	**0.994**

D: degree of nodes, Eg: global efficiency, C: clustering coefficient

lower than for combined attributes. Although using the degree of nodes as a feature also guaranteed good results, the feature of combined attributes was more efficient in classification. Thus, it could be seen that the global efficiency and the clustering coefficient were added into the feature vector as an augmentation index, which was favorable for classification.

The BCI, Motor, NMK and DRI data included 9, 14, 20 and 12 subjects, respectively. In the four data sets, NMK contained the largest number of subjects. Its accuracy rate was the lowest. It could be inferred that for a bigger sample of subjects there would be a bigger chance that two persons might have close values of the discrimination parameters.

4.3. Classification results. For each data set, we adopted 2-fold cross validation and randomly divided the samples into the test set and the training set. Ten times tests were performed. Then, average values were computed. Table 2 summarized classification accuracies of the four data sets in the beta band.

From Table 2 it can be observed that for the BCI, DRI and Motor data the accuracies were ten times all above 0.99; for NMK data, they were also above 0.95. Meanwhile, the fluctuation in classification accuracies was very small. The results showed that the features consisting of brain network attributes were effective in personal identification for different data sets.

To further verify the advantage of the features used in this paper, a fixed feature comprising AR parameters, and the power spectral density (PSD) was used for comparison (Poulos *et al.*, 1999; Hema *et al.*, 2009; Su *et al.*, 2010). This feature was employed to identify the three datasets in the paper. The comparison results are shown in Table 3. They demonstrate that the accuracies of AR parameters were lower than those of the brain network attributes. For the three datasets, the brain network attributes obtained good recognition rates, while the accuracy of fixed parameters used in BCI data was higher than in the case of the other two datasets.

Besides, the recognition accuracy of the BCI data was compared with the results of Nguyen *et al.* (2012), who used Mel-frequency cepstral coefficients as features and the identification accuracy was 0.46 on Graz A 2008 data, which we named BCI data. Clearly, the limitation of their methods did not exist in our approach.

5. Conclusion

This paper proposed an EEG-based method to estimate cognitive phenotypes in personal identification. In contrast to related works, we used properties based on a brain functional network to extract feature vectors. We evaluated the method with four datasets involving different cognitive tasks. Their classification accuracies were all higher than 0.95. Even for a fatigue driving task, in which subjects were required to execute a complex

Table 2. Classification results of the four data sets.

k	BCI data	DRI data	NMK data	Motor data
1	1	1	0.944	1
2	0.986	0.990	0.963	1
3	1	1	0.956	1
4	0.972	0.990	0.950	1
5	0.972	0.979	0.944	0.982
6	0.986	1	0.981	0.964
7	1	0.989	0.963	1
8	1	0.989	0.944	0.991
9	1	0.969	0.956	1
10	1	1	0.963	1
Average	0.992 ± 0.01	0.991 ± 0.01	0.956 ± 0.01	0.994 ± 0.01

task, the method also achieved good performance. Each individual's brain network attributes are unique. We also found that the EEG signals extracted from the beta and gamma bands were much more expressive through the perspective of brain networks. The results indicated that attributes of brain networks could be effective features for personal identification.

Acknowledgment

The authors wish to thank the editor and anonymous referees for their helpful comments for improving the quality of this paper. This work was supported by the National Natural Science Foundation of China (61671193, 61602140), the Science and Technology Program of Zhejiang Province (2018C04012, 2017C33049), and the science and technology platform construction project of the Fujian Science and Technology Department (2015Y2001).

References

Armstrong, B.C., Ruiz-Blondet, M.V., Khalifian, N., Kurtz, K.J., Jin, Z. and Laszlo, S. (2015). Brainprint: Assessing the uniqueness, collectability, and permanence of a novel method for ERP biometrics, *Neurocomputing* **166**(2015): 59–67.

Boccaletti, S., Latora, V., Moreno, Y., Chavez, M. and Hwang, D.U. (2006). Complex networks: Structure and dynamics, *Physics Reports* **424**(4C5): 175–308.

Brunner, C., Leeb, R., Müller-Putz, G., Schlögl, A. and Pfurtscheller, G. (2008). *BCI Competition 2008—Graz data set A*, Graz University of Technology, Graz, `http://www.bbci.de/competition/iv/desc_2a.pdf`.

Bullmore, E. and Sporns, O. (2009). Complex brain networks: Graph theoretical analysis of structural and functional systems, *Nature Reviews Neuroscience* **10**(3): 186–198.

Chavez, M., Valencia, M., Latora, V. and Martinerie, J. (2010). Complex networks: New trends for the analysis of brain connectivity, *International Journal of Bifurcation & Chaos* **20**(6): 1677–1686.

Das, K., Zhang, S., Giesbrecht, B. and Eckstein, M.P. (2009). Using rapid visually evoked EEG activity for person identification, *2009 Annual International Conference of the IEEE Engineering in Medicine and Biology Society, Minneapolis, MN, USA*, pp. 2490–2493.

Fries, P. (2005). A mechanism for cognitive dynamics: Neuronal communication through neuronal coherence, *Trends in Cognitive Sciences* **9**(10): 474.

Hebb, D.O. (2013). *The Organization of Behavior: A Neuropsychological Theory*, John Wiley/Chapman & Hall, Hoboken, NJ.

Hema, C.R., Paulraj, M.P. and Kaur, H. (2009). Brain signatures: A modality for biometric authentication, *International Conference on Electronic Design, Penang, Malaysia*, pp. 1–4.

Huang, X., Altahat, S., Tran, D. and Sharma, D. (2012). Human identification with electroencephalogram (EEG) signal processing, *International Symposium on Communications and Information Technologies, Gold Coast, Australia*, pp. 1021–1026.

Jain, A.K., Bolle, R. and Pankanti, S. (2005). *Biometrics: Personal Identification in Networked Society*, Springer-Verlag New York, New York, NY.

Jamal, W., Das, S., Maharatna, K., Pan, I. and Kuyucu, D. (2015). Brain connectivity analysis from EEG signals using stable phase-synchronized states during face perception tasks, *Physica A: Statistical Mechanics and Its Applications* **434**(2015): 273–295.

Kim, T.K., Kim, H., Hwang, W. and Kee, S.C. (2003). Face description based on decomposition and combining of a facial space with LDA, *International Conference on Image Processing, ICIP 2003, Barcelona, Spain*, pp. 877–880.

Kong, W., Lin, W., Babiloni, F., Hu, S. and Borghini, G. (2015). Investigating driver fatigue versus alertness using the Granger causality network, *Sensors* **15**(8): 19181–19198.

Kong, W., Zhao, X., Hu, S., Vecchiato, G. and Babiloni, F. (2013). Electronic evaluation for video commercials by impression index, *Cognitive Neurodynamics* **7**(6): 531–535.

Kong, W., Zhou, Z., Jiang, B., Babiloni, F. and Borghini, G. (2017). Assessment of driving fatigue based on

intra/inter-region phase synchronization, *Neurocomputing* **219**(2017): 474–482.

Latora, V. and Marchiori, M. (2001). Efficient behavior of small-world networks, *Physical Review Letters* **87**(19): 198701.

Le, V.Q.M., Foucher, J., Lachaux, J., Rodriguez, E., Lutz, A., Martinerie, J. and Varela, F.J. (2001). Comparison of Hilbert transform and wavelet methods for the analysis of neuronal synchrony, *Journal of Neuroscience Methods* **111**(2): 83–98.

Lei, G., Yao, W., Hongli, Y., Ning, Y. and Ying, L. (2014). Study of brain functional network based on sample entropy of EEG under magnetic stimulation at PC6 acupoint, *Biomedical Materials and Engineering* **24**(1): 1063–9.

Ling, W., Li, Y., Yang, X., Xue, Q. and Wang, Y. (2015). Altered characteristic of brain networks in mild cognitive impairment during a selective attention task: An EEG study, *International Journal of Psychophysiology* **98**(1): 8–16.

Maiorana, E., Rocca, D.L. and Campisi, P. (2015). Eigenbrains and eigentensorbrains: Parsimonious bases for EEG biometrics, *Neurocomputing* **171**(2016): 638–648.

McFarland, D.J., McCane, L.M., David, S.V. and Wolpaw, J.R. (1997). Spatial filter selection for EEG-based communication, *Electroencephalography & Clinical Neurophysiology* **103**(3): 386–394.

Nguyen, P., Tran, D., Huang, X. and Sharma, D. (2012). A proposed feature extraction method for EEG-based person identification, *Proceedings of the 2012 International Conference on Artificial Intelligence, Las Vegas, NV, USA*, pp. 1–6.

Onnela, J.P., Saramäki, J., Kertész, J. and Kaski, K. (2005). Intensity and coherence of motifs in weighted complex networks, *Physical Review E* **71**(6 Pt 2): 065103.

Paranjape, R.B., Mahovsky, J., Benedicenti, L. and Koles, Z. (2001). The electroencephalogram as a biometric, *Canadian Conference on Electrical and Computer Engineering, Haran Karmaker, Toronto*, Vol. 2, pp. 1363–1366.

Park, H.J. and Friston, K. (2013). Structural and functional brain networks: from connections to cognition, *Science* **342**(6158): 1238411.

Peng, Y. and Lu, B.-L. (2017). Discriminative extreme learning machine with supervised sparsity preserving for image classification, *Neurocomputing* **261**(2017): 242–252.

Pfurtscheller, G. and Neuper, C. (2001). Motor imagery and direct brain-computer communication, *Proceedings of the IEEE* **89**(7): 1123–1134.

Poulos, M., Rangoussi, M. and Alexandris, N. (1999). Neural network based person identification using EEG features, *IEEE International Conference on Acoustics, Speech, and Signal Processing, Phoenix, AZ, USA*, pp. 1117–1120.

Pujol, F.A., Mora, H. and Girona-Selva, J.A. (2016). A connectionist computational method for face recognition, *International Journal of Applied Mathematics and Computer Science* **26**(2): 451–465, DOI: 10.1515/amcs-2016-0032.

Rosenblum, M.G., Pikovsky, A.S. and Kurths, J. (1996). Phase synchronization of chaotic oscillators, *Physical Review Letters* **76**(11): 1804.

Rosenblum, M.G., Pikovsky, A.S. and Kurths, J. (2012). Synchronization approach to analysis of biological systems, *Fluctuation & Noise Letters* **04**(1): L53–L62.

Rubinov, M. and Sporns, O. (2009). Complex network measures of brain connectivity: Uses and interpretations, *Neuroimage* **52**(3): 1059–1069.

Sakkalis, V., Oikonomou, T., Tsiaras, V. and Tollis, I. (2015). Graph-theoretic indices of evaluating brain network synchronization: Application in an alcoholism paradigm, *Neuromethods* **91**(2015): 159–169.

Saramäki, J., Kivelä, M., Onnela, J.-P., Kaski, K. and Kertész, J. (2007). Generalizations of the clustering coefficient to weighted complex networks, *Physical Review E: Statistical, Nonlinear, and Soft Matter Physics* **75**(2 Pt 2): 027105.

Stam, C.J. (2009). *From Synchronisation to Networks: Assessment of Functional Connectivity in the Brain*, Springer New York, New York, NY.

Steyrl, D., Scherer, R., Faller, J. and Müller-Putz, G.R. (2016). Random forests in non-invasive sensorimotor rhythm brain-computer interfaces: A practical and convenient non-linear classifier, *Biomedical Engineering/Biomedizinische Technik* **61**(1): 77–86.

Su, F., Xia, L., Cai, A. and Ma, J. (2010). Evaluation of recording factors in EEG-based personal identification: A vital step in real implementations, *IEEE International Conference on Systems, Man and Cybernetics, Istanbul, Turkey*, pp. 3861–3866.

Vukašinović, V., Šilc, J. and Škrekovski, R. (2014). Modeling acquaintance networks based on balance theory, *International Journal of Applied Mathematics and Computer Science* **24**(3): 683–696, DOI: 10.2478/amcs-2014-0050.

Ye, J., Janardan, R. and Li, Q. (2004). Two-dimensional linear discriminant analysis, *Photogrammetric Engineering & Remote Sensing* **5**(6): 1431–1441.

Yeom, S.K., Suk, H.I. and Lee, S.W. (2013). Person authentication from neural activity of face-specific visual self-representation, *Pattern Recognition* **46**(4): 1159–1169.

Wanzeng Kong received both the BSc and PhD degrees from the Electrical Engineering Department, Zhejiang University, Hangzhou, China, in 2003 and 2008, respectively. He is currently a professor and a vice-dean of the College of Computer Science, Hangzhou Dianzi University. His research interests include cognitive computing, pattern recognition and BCI-based electronic systems. Dr. Kong is also a member of the IEEE, ACM and CCF.

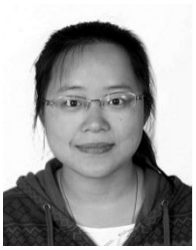

Bei Jiang received her BSc degree in information management and information systems from Zhejiang Gongshang University, Hangzhou, China, in 2014. She received her MSc degree in computer application technologies at the College of Computer Science of Hanghzou Dianzi University in 2017. Currently, she is an engineer in the R&D department of Nokia Shanghai Bell. Her main research interests include deep learning, brain networks.

Qiaonan Fan received her BSc degree in information and computing sciences from Yancheng Teachers University, Jiangsu, China, in 2016. She is now studying for her MSc degree in computer technology at the College of Computer Science of Hanghzou Dianzi University. Her main research interests are in pattern recognition.

Li Zhu is a PhD student in the Cognitive Science Department at Xiamen University, China, and has been selected a member of international participant associates in RIKEN, Japan. She has worked on signal processing, time series analysis and high-dimensional data processing.

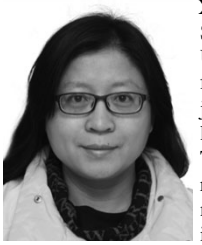

Xuehui Wei received her is BSc degree from the School of Mathematics and Statistics, Ludong University, Yantai, China, in 2003, and the PhD from the School of Mathematical Science, Zhejiang University, Hangzhou, China. She is now a lecturer in the School of Computer Science and Technology, Hangzhou Dianzi University. Her research interests include image quality assessment, visual perception and cognitive computing.

Received: 26 May 2017
Revised: 20 November 2017
Re-revised: 7 March 2018
Accepted: 20 March 2018